Rare Metal Materials and Engineering
Volume 48, Issue 3, March 2019
Available online at www.rmme.ac.cn

Science Press

Cite this article as: Rare Metal Materials and Engineering, 2019, 48(3): 0716-0720.

ARTICLE

DIC/EBSD Coupling Analysis of Microstructure Evolution and Strain Localization During Bending of Al-Li Alloy

Jin Xiao[1, 2], Zhang Guodong [1], Xue Fei[1], Zhao Yanfen[1], Liu Wenbo [2, 3]

[1] Suzhou Nuclear Power Research Institute, Suzhou 215004, China; [2] Tsinghua University, Beijing 100084, China; [3] Shaanxi Key Laboratory of Advanced Nuclear Energy and Technology, Xi'an Jiaotong University, Xi'an 710049, China

Abstract: The damage mechanism of commercial 2060 (T8) aluminum alloy during bending was studied. The microstructure evolution and strain localization were investigated by scanning electron microscope (SEM), electron backscattered diffraction (EBSD) and digital image correlation (DIC) methods. A new method based on the dispersion distribution of copper powders was developed, which can be used to simultaneously characterize the strain distribution and microstructure evolution of the same region. The experimental results show that the macro shear band is formed during the bending, and the crack grows along the macro shear band. This phenomenon can be attributed to the larger volume fraction of small angle grain boundaries (SAGBs) formed in the macro shear band, and less energy is needed if the crack propagates in the direction of macro shear bands.

Key words: Al-Li alloy; deformation; microstructure; fracture

Al-Li alloy is one of the most potential structure materials for aerospace structures due to its excellent properties such as high strength and low density. As a third generation of Al-Li alloy, 2060 alloy has the advantages in elastic modulus, fatigue crack growth resistance, corrosion resistance, plane stress, fracture toughness and density compared with the first and second generation products[1-3]. It has been successfully applied to the commercial aircraft C919 in China [4].

One of the key steps in the application of 2060 aluminum alloy is to process the commercial sheets into the desired shape, and the most common way is bending. It is found that the macro shear bands formed during bending are harmful to the reliability of the material [5-8]. In the past several decades, some attention have been paid to the formation of macro shear bands during bending. It is reported that the formation of macro shear bands can be affected by the precipitates, crystallographic orientation and alloy composition[9-11]. It is believed that the crack starts at the maximum region in the macro shear band and grows in the same direction as the shear band at the early period[6,9,12]. However, most of the theories are about the surface roughness or strain localization causing damage, and the shear band is still difficult to express due to the limitations of traditional characterization techniques[5]. In addition, these studies can observe the morphology of macro shear band but cannot describe the change of strain until the application of DIC techniques.

The present work aims to find out the microstructural differences between the inside and the outside of the macro shear band by the DIC and EBSD combined characterization techniques, which is the first study applied in 2060 alloy during the bending. The relationship between microstructural differences and macro shear band was analyzed, and the mechanism of crack propagation during bending was also discussed.

1 Experiment

In the present study, the material used was 2060 aluminum alloy commercially manufactured by Alcoa, Inc., and the heat treatment was T8. The composition of the studied alloy was analyzed by infrared spectrometry (IR).

A split sample of 10 mm×3 mm×2 mm (along the rolling direction (RD), transverse direction (TD), and normal direc-

Received date: March 11, 2018
Foundation item: National Key Research and Development Program of China (2016YFC0801905); National Natural Science Foundation of China (11705137)
Corresponding author: Liu Wenbo, Ph. D., Department of Nuclear Science and Technology, Shaanxi Key Laboratory of Advanced Nuclear Energy and Technology, Xi'an Jiaotong University, Xi'an 710049, P. R. China, E-mail: liuwenbo@xjtu.edu.cn

tion (ND)) was used. The upper surfaces (RD×ND) of the specimens for characterization were first mechanically ground and then electropolished in $HClO_4$:C_2H_5OH=10:90 (*v*/*v*) solution at room temperature for 15~20 s under an applied voltage of 20 V.

Electron backscatter diffraction (EBSD) data were collected using an Oxford Nordly 2 (Oxford Instruments, Oxford, England), which was operated at an accelerating voltage of 20 kV, a magnification of 300×, a working distance of 15 mm, and a tilt angle of 70°. The EBSD probe scan was performed using a 2 μm step size over the same area as the scanning electron microscopy (SEM) scan.

Fig. 1 shows the grain structure of 2060 alloy characterized by EBSD along the full cross-section[8], which shows a typical pancake-shaped grain structure with a partial recrystallization. The grains are significantly flattened and elongated in the rolling direction, and the size near the surfaces is larger than that in the middle of the specimen.

The DIC system has been successfully used to characterize the strain evolution during bending (where data are recorded at different stages of bending of a specimen and later used as an input to the DIC system for strain calculation)[6-8], and is an effective method for measuring the strain distribution. According to the principle of strain calculation used in this study, the Cu powder was used as random speckle patterns with an average size of 1 μm. The Cu powder was dispersed in ethanol and treated in an ultrasonic device for 15 min until the uniform dispersion of the powder, and then the copper powder ethanol suspension was taken to the surface of the sample by a pipette. After the alcohol was completely volatilized, a large number of dispersed copper powder particles with different sizes were formed on the surface of the SEM sample. However, in backscattered electron (BSE) images, the matrix (black) and powder particles (white patterns with different sizes) clearly contrast because different elements are imaged differently for this technique. Thus, the powder particles appear as a speckle pattern for strain calculations, as shown in Fig. 2a and 2b.

In this study, a commercially available DIC system (VIC-2D, CSI, USA) was used. Images processed by the DIC system were collected by a BSE probe installed in a Tescan MIRA3 scanning electron microscope (Tenscan, Brno, Czech Republic).

The microbending jig is designed and produced on the basis of the manually operated screw-driven micro jig designed by Davidkov et al[12], and a few improvement is made for the use in similar bending experiments. Semicircular punches and dies with different bending radii were used instead of a V-shaped punch. The radii of punches (*r*) are 10, 5, and 3 mm, whereas the radii of dies are 12, 7, and 5 mm; the radii of the punches are 2 mm smaller than the radii of their corresponding dies, so as to avoid damaging the plates during forming.

Table 1 Chemical composition of 2060 alloy (wt%)

Ag	Cu	Fe	Mg	Mn	Si	Ti	Zn	Zr	Li	Al
0.34	3.52	0.03	0.66	0.29	0.02	0.03	0.34	0.1	0.73	Bal.

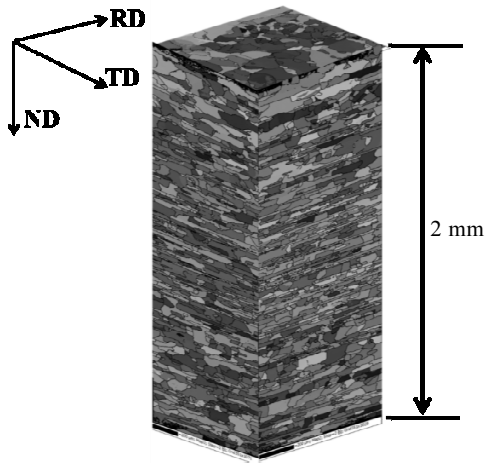

Fig. 1 Triplanar EBSD micrograph of 2060-T8 alloy with microstructural features[8]

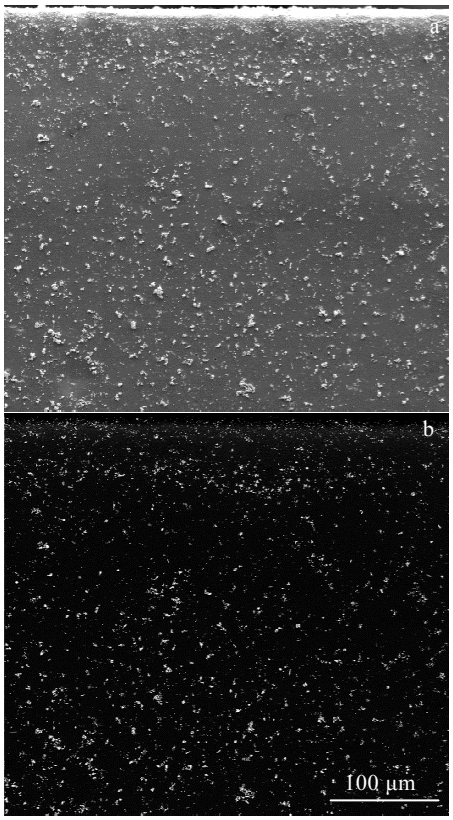

Fig. 2 Microstructures of surface with copper powders: (a) SEI and (b) BSEI

The punches and dies can be replaced during the experiments. This method enables quantitative descriptions of the bending radii of specimens.

The bend line is perpendicular to the RD and parallel to the TD. Each specimen was bent from 10 mm to 3 mm, and the same region was observed during bending.

2 Results and Discussion

2.1 Distribution of strain during bending

Fig. 3 shows the features of specimen surface under different bend radii. As shown in Fig. 3a, the surface of the sample is smoothed before bending. A radian outside the specimen is observed when the bending radius reaches 10 mm (Fig. 3b). The radian is more obvious and some depressions appear in the radian when the bending radius reaches 5 mm (Fig. 3c). However, no defect, such as crack or void, is observed on the specimen. The embossed phenomenon is clearly observed in the surface of specimen, when the bending radius reaches 3 mm (Fig. 3d). Under this bending condition, the crack appears outside the specimen, which can be clearly seen in the red frame shown in Fig. 3d.

From the four images in Fig. 3, it can be found that there is almost no change in the size and position of the copper powders, which means that the features of the dispersed copper powders are stable during the bending and can be used as a speckle pattern. This method of using copper powders is more applicable than using the precipitates as speckle patterns, for not all materials have enough suitable precipitates in size and distribution. It is easy to remove the speckle patterns and not damage the specimen surface, making it simple and feasible to combine the surface strain measurement of the sample with the microstructure characterization of EBSD. This can be used to characterize the evolution of the microstructure while observing the surface strain measurement in the same region. It is important to understand the mechanism of the generation and expansion of cracks during the process of deformation.

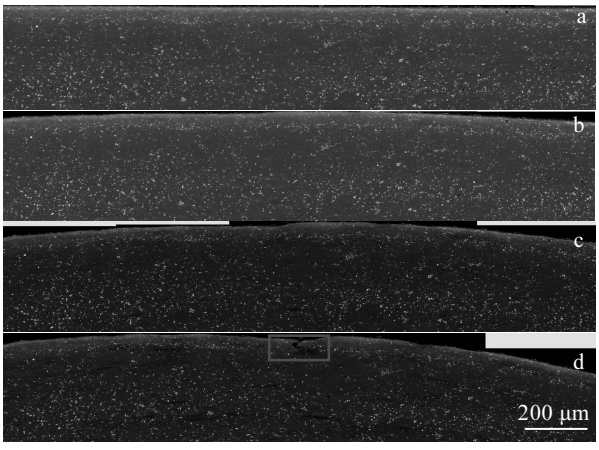

Fig. 3 SEM observation of the bending specimen with different bend radii: (a) r=0, (b) r=10 mm, (c) r=5 mm, and (d) r=3 mm

Fig. 4 shows the strain distribution during bending. The BSE images with different bend radii were input into the DIC software and the figures with strain distribution were calculated. It can be seen in Fig. 4 that there is a significant difference in the distribution of strain. In Fig. 4a, the interested area is signed with dark blue, which means that there is no strain during bending if the color is dark blue (corresponding to the state before bending). When the bend radius reaches 10 mm (Fig. 4b), some areas with light blue appear in the strain distribution map, which means that a larger strain in this area appears and strain localization is observed. However, as shown by the dashed lines in the strain distribution map (Fig. 4c), some macro shear bands are formed when the bend radius reaches 3 mm. At the outer line of the bending sample, the crack starts, and the maximum strain happens at the same area. It can be concluded that the strain localization induces a macro shear band, and the amount of strain in macro shear band decreases from the outside to the inside of the specimen.

There are many theories about the macro shear bands formed during the bending, but there is no clear conclusion to analyze this phenomenon. From the view of stress distribution, the outside of specimen is affected by tensile stress, and the tensile direction of 45° generally has the maximum shear stress. From our experimental results, the angle between the macro shear band and the tensile direction was nearly 45°, and the strain localization or shear strain concentration easily occurs in this region, consequently leading to damage during bending [13,14].

According to mainstream opinions of microstructure evolution, the shear band always occurs during bending, and a simple model proposed by Tvergaard et al [15,16] supposed that an imperfect region existed in the real samples and the reason is complex, which may be affected by many factors in the material, such as direction of force, voids, and orientation of grains. This imperfect region is throughout the whole material, not only the surface. Due to the difference in the flow stress between the imperfect region and perfect region during bending, the stress concentration occurred much more easily in the imperfect region. The flow stress acting on the imperfect region is greater than that acting on the perfect region. Therefore, in the vicinity of the imperfect region, the strain increases faster than that in other regions. During the deformation process, the strain near the defect region reaches a threshold in a short time and macro shear band is formed. In other words, the strength of the imperfect region is weaker than that in other positions of the material itself. Under the same stress conditions, the region is prone to large deformation compared to other regions, resulting in strain concentration and formation of macro shear band [17]. The macro shear band is a manifestation of strain localization of the weaker thin slice during deformation.

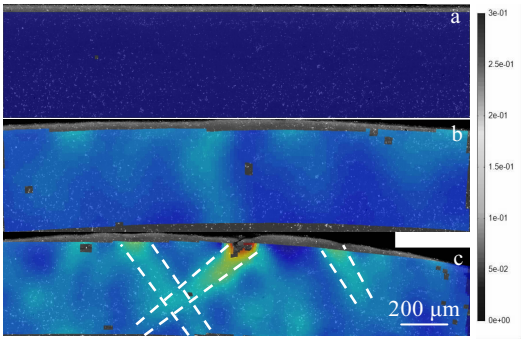

Fig. 4 Strain distribution during bending: (a) r=0, (b) r=10 mm and (c) r=3 mm

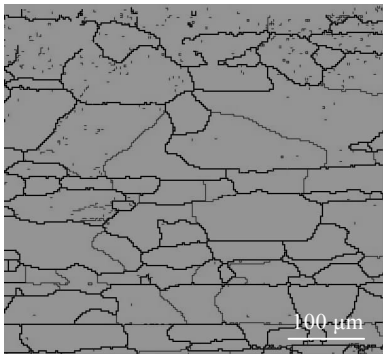

Fig. 5 Grain boundary map before bending

The microstructure of material is not unified due to the small differences in process, and there are some defects such as voids and micro cracks in the material. Therefore, it is difficult to describe and analyze the formation mechanism of macro shear band in the bending process by the current theories, and these theories need to be improved furthermore.

2.2 Microstructure evolution during bending

It has been found that the crack starts in the macro shear band with the maximum strain and grows along the micro shear band, and the microstructure in this region will be changed significantly [7,8]. However, due to the limitations of traditional characterization techniques, it is difficult to find the study of the microstructure of this region.

The grain boundary map using EBSD before bending is shown in Fig. 5. It can be seen that lots of large angle grain boundaries (LAGBs, black lines, more than 15°) and a few small angle grain boundaries (SAGBs, red lines, 2°~15°) are observed in the sample before bending, which means that the grains are in the tempered state and almost no dislocation is observed.

Fig. 6 shows the specimen's strain localization at different bend radii and its corresponding microstructures in the same region. It can be seen that strain stratification occurs on the surface of the sample when the bending radius reaches 10 mm (Fig. 6a). As shown in Fig. 6b, the macro shear band is formed on the surface of the sample when the bending radius reaches 5 mm. Fig. 6c is the grain boundary distribution map when the bending radius reaches 5 mm, and the studied region is the same as the red dashed line area in Fig. 6b. From the image of Fig. 6c, lots of SAGBs can be found in this state. However, more SAGBs can be found in the area of macro shear band, as shown by the blue dashed line in Fig. 6c. Comparing Fig. 6b and Fig. 6c, it is found that the larger the strain, the larger the volume fraction of SAGBs as a whole, which means that grains in the area with larger strain have larger deformation. After the copper power was removed in an ultrasonic cleaning machine and the sample was slightly mechanically polished, the interested region was observed by SEM. Fig. 6d is the SEM image of the crack growth after the bending radius reaches 3 mm, and it can be seen that cracks propagate along the macro shear band, which is the same direction as the propagation of more SAGBs.

Researchers have found that the band structure observed by EBSD is the geometrically necessary boundaries (GNBs) which were observed by TEM in previous studies[18]. The band structure was formed in the process of grain subdivision during deformation, and it is found that the GNBs are almost parallel to the {111} slip plane in grains [19]. A large number

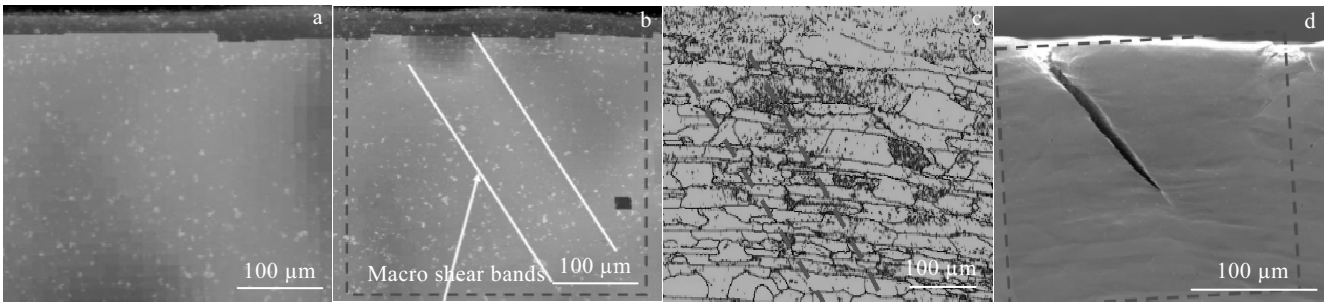

Fig. 6 Strain localization and microstructure evolution at the same region: (a) DIC map of r=10 mm, (b) DIC map of r=5 mm, (c) grain boundary map of r=5 mm, and (d) SEM image of the crack propagation

of SAGBs in grains can be regarded as the subdivision of grains into lots of band structures that are staggered during bending. It is suggested that the crack grows along the {111} slip planes in the initial stage of crack propagation[8]. In general, the crack grows along the direction of lowest energy. Cracks propagating along the SAGBs need less energy than along the LAGBs, which means that SAGBs is the preferred path for crack propagation under the same conditions [20]. In addition, the dislocation concentration in the macro shear band is due to the large degree of deformation, which results in the increased hardness and decreased plasticity, since it is easy to deliver energy by crack.

3 Conclusions

1) A new method based on the dispersion distribution of copper powders is developed, which can be used to characterize the strain distribution and microstructure evolution of the deformation region simultaneously.

2) Macro shear bands form during the bending and the crack grows along the macro shear band. The grains in the macro shear band have more SAGBs, and the crack propagates in the direction of macro shear bands with more SAGBs, since less energy is required if the crack propagates along this direction.

References

1 Rioja Roberto J, Liu John. *Metallurgical and Materials Transactions A*[J], 2012, 43(9): 3325

2 Karabin L M, Bray G H, Rioja R J *et al. ICAA13: 13th International Conference on Aluminum Alloys*[C]. John Wiley Sons Inc, 2013

3 Zheng Ziqiao, Li Jingfeng, Cheng Zhiguo *et al. The Chinese Journal of Nonferrous Metals*[J], 2011, 21: 2337 (in Chinese)

4 Yang Yongbiao, Zhang Zhimin, Zhang Xing. *Materials Science Forum*[J], 2015, 816: 810

5 Becker R. *Journal of Applied Mechanics*[J], 1992, 59(3): 491

6 Davidkov A, Jain M K, Petrov R H *et al. Materials Science and Engineering A*[J], 2012, 550(30): 395

7 Mattei Laurent, Daniel Dominique, Guiglionda Gilles *et al*. *Materials Science and Engineering A*[J], 2013, 559: 812

8 Jin Xiao, Fu Baoqin, Zhang Chenglu *et al. International Journal of Minerals, Metallurgy, and Materials*[J], 2015, 22(12): 1313

9 Marzouk M, Jain M, Shankar S. *Materials Science and Engineering A*[J], 2014, 598: 277

10 Ikawa Shingo, Asano Mineo, Kuroda Mitsutoshi *et al. Materials Science and Engineering A*[J], 2011, 528(12): 4050

11 Hu X H, Jain M, Wu P D *et al. Journal of Materials Processing Technology*[J], 2010, 210(9): 1232

12 Davidkov Aleksandar, Petrov Roumen H, Smet Peter De *et al*. *Materials Science and Engineering A*[J], 2011, 528(22-23): 7068

13 Pan Jinsheng, Tong Jiangmin, Tian Minbo. *Foundamental of Materials Science*[M]. Beijing: Tingshua Press, 1998 (in Chinese)

14 Li Junfeng, Zhang Xiong. *Theoretical Mechanics*[M]. Beijing: Tingshua Press, 2010 (in Chinese)

15 Kuroda M, Tvergaard V. *International Journal of Plasticity*[J], 2007, 23(2): 244

16 Harren S V, Lowe T C, Asaro R J. *Philosophical Transactions of the Royal Society of London*[J], 1989, 328: 443

17 Tvergaard V, Needleman A. *Proceedings of the Royal Society A*[J], 1993, 443: 547

18 Liu Q, Hansen N. *Proceedings of the Royal Society A*[J], 1998, 454: 2555

19 Jin Xiao, Fu Baoqin, Zhang Chenglu *et al*. *Acta Metallurgica Sinica* [J], 2015, 28: 1149

20 Cheng Yuanyuan, Zheng Ziqiao, Cai Biao *et al. Rare Metal Materials & Engineering*[J], 2011, 40(11): 1926 (in Chinese)

Al-Li 合金弯曲过程中微观组织结构演变与应变集中的 DIC/EBSD 耦合分析

金 晓[1,2]，张国栋[1]，薛 飞[1]，赵彦芬[1]，柳文波[2,3]

(1. 苏州热工研究院有限公司，江苏 苏州 215004)

(2. 清华大学，北京 100084)

(3. 西安交通大学 陕西省先进核能技术重点实验室，陕西 西安 710049)

摘 要：通过扫描电镜(SEM)、电子背散射(EBSD)和数字图像相关方法(digital image correlation, DIC) 相结合的方法对 2060-T8 铝合金在弯曲变形过程中微观组织结构进行表征并对其损伤机制进行了研究。基于 DIC 和 EBSD 准原位技术，发展了一种以弥散分布的铜粉末为标记点的同一区域应变测量和微观结构表征技术。实验结果显示合金在弯曲过程中形成了宏观剪切带且裂纹的扩展也是沿着宏观剪切带进行，发现造成这种现象的原因是由于在形变过程中在宏观剪切带上产生了大量的小角晶界 (SAGBs)，而裂纹沿小角晶界富集的地方进行扩展所需的能量相对是最小的。

关键词：Al-Li合金；变形；微观结构；断裂

作者简介：金 晓，男，1986 年生，博士，苏州热工研究院有限公司，江苏 苏州 215004，电话：0512-65357705，E-mail: jin_xiao2002@163.com